A Simple Method for Determining Fault Location on Distribution Lines

Thomas Covington, Tim Stankiewicz, and Rick Anderson
Fayetteville Public Works Commission

Larry Wright and Brett Cockerham
Schweitzer Engineering Laboratories, Inc.

Presented at the
44th Annual Western Protective Relay Conference
Spokane, Washington
October 17–19, 2017

Previously presented at the
4th Annual PAC World Americas Conference, August 2017

Previous revised edition released May 2017

Originally published in the
proceedings of the 71st Annual Georgia Tech
Protective Relaying Conference as an alternate, May 2017

A Simple Method for Determining Fault Location on Distribution Lines

Thomas Covington, Tim Stankiewicz, and Rick Anderson, *Fayetteville Public Works Commission*
Larry Wright and Brett Cockerham, *Schweitzer Engineering Laboratories, Inc.*

***Abstract*—Different methods for finding the location of a fault on a distribution line have been available for some time. These methods include the use of faulted circuit indicators and checking the fault current recorded during a trip. With the advent of the microprocessor-based relay, impedance-based fault location became prevalent. It is difficult, however, to use impedance-based fault location on distribution lines because the distribution system is nonhomogeneous, consisting of various pole configurations, wire sizes, and taps. Automated methods have been developed to locate faults on distribution lines; however, these methods may not be cost-justifiable for small municipal and cooperative utilities.**

Fayetteville Public Works Commission (PWC) in Fayetteville, North Carolina, undertook a pilot project to implement a simple method for determining fault location using fault location information from their protective relays and a simple spreadsheet to pinpoint the fault location on their distribution feeders. This paper examines the methods available for fault location and describes the method employed at Fayetteville PWC. It shares the results of their pilot project, including the accuracy of their fault location method for actual faults and the amount of time required to find those faults. This paper provides readers the information to implement Fayetteville PWC's fault location system on their own distribution system.

I. Introduction

Fayetteville Public Works Commission (PWC) is a municipally owned transmission, distribution, and generation utility serving over 82,000 customers in Fayetteville, North Carolina. The engineers at both Fayetteville PWC and the City of Wilson, North Carolina, have had some success over the years predicting fault location on their respective systems based on current magnitude. They did this using spreadsheets that provided a simple model of their power system and the available fault currents for different types of faults along their distribution circuits.

With the advent of the microprocessor-based relay, impedance-based fault location became prevalent. As described in Section II, impedance-based fault location methods have evolved that practically remove the effect of fault resistance and provide more accurate fault location, which cannot be done by looking at fault current magnitude alone. Impedance-based fault location is relatively simple to use on a transmission line. However, it is difficult to use on distribution lines because the distribution system is nonhomogeneous; it consists of various pole configurations, wire sizes, and taps. Some utilities have employed centralized automated schemes for determining fault location in the distribution system [1]; however, this may be out of reach for the small utility. At least one other utility has modeled their lines using a spreadsheet in order to better locate faults [2].

In the fall of 2015, Fayetteville PWC won a grant from the Demonstration of Energy & Efficiency Developments (DEED) Program of the American Public Power Association (APPA) to "develop a simple method to help small to medium public power utilities locate electrical faults using off the shelf hardware, power transformer characteristics and distribution line impedance" [3]. This paper documents some of that effort and demonstrates how a utility can implement Fayetteville PWC's fault location system on their own distribution system.

II. Fault Location Methods

Several methods for identifying the location of a faulted line segment have been discussed in various literature [1] [2] [4] [5] [6] [7]. The fault current magnitude, simple impedance, and modified Takagi impedance methods are discussed in this paper.

A. Fault Current Magnitude Method

Every electrical engineer knows that V = IZ. Knowing that the fault current on a line is dependent on the location of the fault along that impedance, Z, engineers and technicians have long used current magnitude to estimate the distance to the fault. Before the advent of digital relays, an electromechanical device known as the annunciator-type ammeter (shown in Fig. 1) was applied to help identify the fault location [4].

Fig. 1. Annunciator-Type Ammeter

The annunciator-type ammeter displayed the approximate magnitude of fault currents using calibrated targets that

flipped up to indicate that a level of current was exceeded. The identified target could then be referenced against fault calculations that showed the magnitude of fault current at various points along the line.

Similar methods can be applied using microprocessor-based relays. On distribution systems, it is still common practice for an engineer or technician to check the fault current displayed on the front panel of a relay or recloser control to estimate the distance to a fault, much in the same way as with the annunciator-type ammeter. Some current-based methods are more sophisticated than reviewing the front panel. Reference [5] describes a method to estimate the fault location using the source and line impedances along with the magnitude of the measured fault current. The method applies a quadratic equation to interpolate the fault distance. Alternatively, if the fault current profile is available, several points could be used to apply an equation that best fits the simulated data, as opposed to using a quadratic equation. Applying this equation also yields a fault location as a function of the measured current, although perhaps a bit more accurately.

B. Simple Impedance Method

Microprocessor-based transmission relays typically use an impedance-based method to locate faults. This feature was even included in the very first commercially available microprocessor-based distance relays. As discussed throughout [5], identifying the fault type is crucial for determining an accurate fault distance. The involved phase(s) dictates which measurements to use within the distance-to-fault calculations. A single-ended, impedance-based method can approximate the distance to the fault using the current and voltage of the involved phase(s), the zero- and positive-sequence line impedance, and the zero-sequence current [5]. This can be represented with a simple equation for estimating the distance to the fault, as shown in (1).

$$V_S = m \bullet Z_{1L} \bullet I_S \tag{1}$$

where:

m = per-unit distance to the fault (%).

Z_{1L} = positive-sequence line impedance (Ω).

V_S = voltage measured at the relay (V).

I_S = current measured at the relay (A).

The one-line diagram in Fig. 2 illustrates this concept.

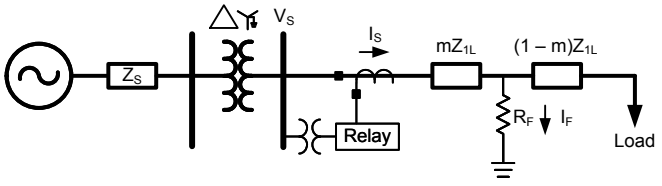

Fig. 2. One-Line Diagram

Equation (1) uses the fundamental concept of Ohm's law to estimate the fault distance. Table I demonstrates the expansion of V_S and I_S, respectively, by fault type.

TABLE I
SIMPLE IMPEDANCE METHOD FOR DETERMINING FAULT LOCATION

Fault Type	Vs	Is
A-G	V_a	$I_a + I_0 \bullet 3 \bullet k$
B-G	V_b	$I_b + I_0 \bullet 3 \bullet k$
C-G	V_c	$I_c + I_0 \bullet 3 \bullet k$
A-B, A-B-G, A-B-C	V_{ab}	I_{ab}
B-C, B-C-G, A-B-C	V_{bc}	I_{bc}
C-A, C-A-G, A-B-C	V_{ca}	I_{ca}

where:

$k = (Z_{0L} – Z_{1L})/3 \bullet Z_{1L}$.

Z_{0L} = zero-sequence line impedance.

I_0 = zero-sequence current.

Also, it is important to note that (1) neglects the influence of fault resistance. Equation (1) can be further enhanced by including both the fault resistance, R_F, and fault current, I_F, as shown in (2).

$$V_S = m \bullet Z_{1L} \bullet I_S + R_F I_F \tag{2}$$

The per-unit fault distance can then be determined by solving for *m* if the quantities R_F and I_F are known, as shown in (3).

$$m = \frac{V_S - R_F I_F}{Z_{1L} \bullet I_S} \tag{3}$$

However, R_F and I_F are typically unknown.

C. Modified Takagi Method

The modified Takagi method removes the two unknown terms (R_F and I_F) from the fault location calculation by multiplying (3) by the complex conjugate of I_0 and saving only the imaginary components. First, the modification can be understood better by restructuring (3) as (4).

$$m = \frac{V_S}{Z_{1L} \bullet I_S} - \frac{R_F I_F}{Z_{1L} \bullet I_S} \tag{4}$$

The modified Takagi method removes the effects of load current by multiplying (4) by the complex conjugate of the measured zero-sequence current, as shown in (5), and only the imaginary portion is preserved.

$$m = \frac{\mathrm{Im}\left(V_S \bullet 3 \bullet I_0^*\right)}{\mathrm{Im}\left(Z_{1L} \bullet I_S \bullet 3 \bullet I_0^*\right)} - \frac{\mathrm{Im}\left(R_F I_F \bullet 3 \bullet I_0^*\right)}{\mathrm{Im}\left(Z_{1L} \bullet I_S \bullet 3 \bullet I_0^*\right)} \tag{5}$$

Recall that zero-sequence current is an effective quantity for ground faults. In addition, while preserving only the imaginary portion, (5) can be further simplified. There is no imaginary component within resistance; therefore, the I_F and $3I_0$ terms evaluate to zero. This yields (6).

$$m = \frac{\mathrm{Im}\left(V_S \bullet 3 \bullet I_0^*\right)}{\mathrm{Im}\left(Z_{1L} \bullet I_S \bullet 3 \bullet I_0^*\right)} \tag{6}$$

The single-ended, modified Takagi method, shown in (6), allows for a simple approach to eliminate the effects of both load and fault resistance.

The current magnitude method is attractive because it is simple and makes no assumptions about the line being homogeneous. However, accuracy is affected when the fault has some resistance. The modified Takagi method, on the other hand, accounts for fault resistance but assumes a homogeneous line. The impact to the modified Takagi method becomes more pronounced as different conductor sizes are used. If only conductors of similar X/R ratio are between the substation and the fault, the impact of the non-homogeneity of the conductors will be minimal. To get the best of both worlds, the method described in Section IV includes both the current-based and impedance-based methods to help determine fault location.

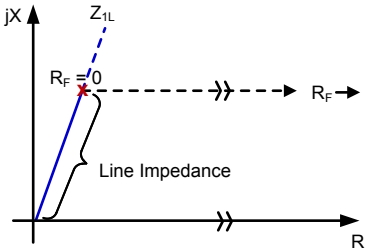

Fig. 3. Single-Ended, Modified Takagi Method

III. Information Available From the Relay

The relays applied at Fayetteville PWC generate an event report with each trip. The event report includes oscillography showing the instantaneous voltages and currents for 4 cycles pre-trip and 11 cycles post-trip, along with the state of all protective and logic elements in the relay for that period of time. An event summary is also generated, which is what Fayetteville PWC uses to obtain the information they need to locate the fault. Event summaries contain the following information:

- Relay and terminal.
- Date and time the event was triggered.
- Event type.
- Fault location.
- Recloser shot count at the trigger time.
- System frequency at the front of the event report.
- Front-panel fault targets at the time of the trip.
- Phase (IA, IB, and IC), neutral ground (IN), calculated residual ground (IG = 3I0), and negative-sequence (3I2) current magnitudes in amperes primary measured at the largest phase current magnitude in the triggered event report.

Fig. 4 shows an example event summary.

```
FEEDER 1                          Date: 07/12/2016  Time: 09:28:31.721
STATION A

Event: AG T  Location:    2.36  Shot: 0  Frequency:  60.01
Targets: 11100100    01010010
Currents (A Pri), ABCNGQ:   2752      209   209     0  2689  2689
```

Fig. 4. Example Event Summary

The information in the event summary can be gathered in a number of ways: (1) it appears on the front panel of the relay; (2) it is viewed using terminal commands on a connected PC; (3) it is downloaded with the event report; (4) the full summary or just the fault location can be communicated over SCADA.

IV. Data and Calculations in the Fault Location Spreadsheet

The Fayetteville PWC fault calculation Microsoft® Excel® spreadsheet has several sections for data entry and calculations. These sections include transformer data, conductor impedance data, system model, fault currents, and impedance-based fault location. Note that complex math is required, and for Excel to do complex math, the Analysis ToolPack add-in must be installed. The Excel equations for calculations requiring complex math are included in Appendix A.

A. Transformer Data

Transformer data are entered into the spreadsheet in cells C2 through C10, as shown in Fig. 5. These data primarily come from the transformer nameplate. The data with the heavy black borders are entered by the user. All other values are calculated.

	A	B	C
2	Transformer Size (MVA)		20
3	Impedance (Z%)		8.56
4	Voltage Φ-Φ (LV)		13090
5	Voltage Φ-▼ (LV) Grd Y		7560
6	Voltage Φ-▼ (LV) after LTC		7200
7	Voltage (HV) Delta		67000
8	X / R ratio		22.5
9	PT Ratio		60
10	CT Ratio		120
11	Zmagnitude (Ω)		0.73
12	Zcomplex (Ω)		0.0326+0.7326j
13	Ifault (A)		10302

Fig. 5. Transformer Data

The X/R ratio is selected from Fig. 6.

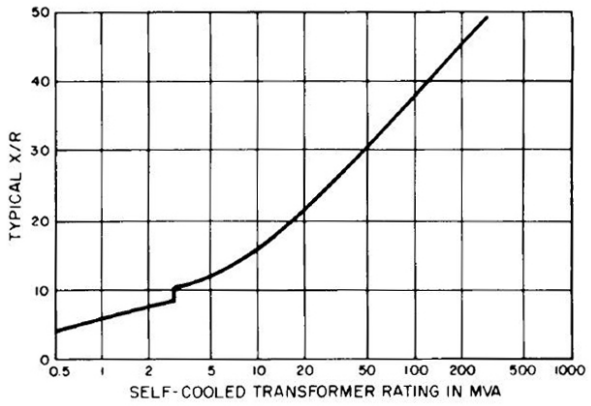

Fig. 6. Transformer X/R Ratios [8]

The spreadsheet shows the calculation of impedance magnitude in primary ohms (C11), the complex impedance

(C12), and the available three-phase fault current (C13). These cells use calculations from (7), (8), and (9), respectively.

$$Z_{magnitude} = \frac{Z\% \bullet (kV_{\Phi-\Phi})^2}{100} \quad (7)$$

$$Z_{complex} = Z_{magnitude} \bullet \left(\cos\left(\tan^{-1}\left(\frac{X}{R}\right)\right) + j\sin\left(\tan^{-1}\left(\frac{X}{R}\right)\right)\right) \quad (8)$$

$$I_{fault} = \frac{MVA \bullet 1000}{3 \bullet kV_{\Phi-\blacktriangledown} \bullet \left(\frac{Z\%}{100}\right)} \quad (9)$$

B. Conductor Impedance Data

Conductor impedance data come from conductor manufacturers' data, as shown in Fig. 7. These data are used in developing the system model. Note that the positive-sequence impedance, Z1, is equal to the negative-sequence impedance, Z2. The zero-sequence impedance, Z0, is also applied for all fault types that include ground.

	A	B	C
15		R+jX)/1000'	
16	Wire Size	Z1 & Z2	Z0
17	477 w/ 4/0-N	.0409+.1167j	.1296+.3576j
18	477 w/ 2/0-N	.0409+.1167j	.1504+.3820j
19	477 w/ 1/0-N	.0409+.1167j	.1614+.4008j
20	355 w/ 4/0-N	.0580+.1206j	.1408+.3615j
21	355 w/ 2/0-N	.0580+.1206j	.1672+.3860j
22	355 w/ 1/0-N	.0580+.1206j	.1784+.4047j
23	2/0AL W/ 2/0-N	.1695+.1566j	.2989+.4595j
24	1/0AL W/ 1/0-N	.2121+.1595j	.3447+.4794j

Fig. 7. Conductor Impedance Data

C. System Model

The system model is built by entering map data from the distribution system. Fayetteville PWC chooses to enter these data in segments of 0.1 miles to correspond to utility truck odometers. The user enters the segment length and wire size in Columns A and C, respectively, as shown in Fig. 8.

	A	B	C
31	Segment Length (miles)	Total Distance (miles)	Wire Size
32			
33	0.1	0.1	477 W/ 4/0-N
34	0.1	0.2	477 W/ 4/0-N
35	0.1	0.3	477 W/ 4/0-N
36	0.1	0.4	477 W/ 4/0-N
37	0.1	0.5	477 W/ 4/0-N
38	0.1	0.6	477 W/ 4/0-N
39	0.1	0.7	477 W/ 4/0-N
40	0.1	0.8	477 W/ 4/0-N
41	0.1	0.9	477 W/ 4/0-N
42	0.1	1.0	477 W/ 4/0-N
43	0.1	1.1	477 W/ 4/0-N
44	0.1	1.2	355 W/ 4/0-N
45	0.1	1.3	355 W/ 4/0-N
46	0.1	1.4	355 W/ 4/0-N
47	0.1	1.5	355 W/ 4/0-N
48	0.1	1.6	355 W/ 4/0-N
49	0.1	1.7	355 W/ 4/0-N

Fig. 8. Circuit Segment Data

From the circuit segment data, the spreadsheet populates the Conductor Impedance/1000' in Columns D and E, as shown in Fig. 9, with the conductor impedance data from Fig. 7. It then multiplies that impedance by the segment length in Column A (Fig. 8) times 5,280 feet per mile divided by 1,000 feet to derive the segment impedance shown in Columns F and G of Fig. 9.

	D	E	F	G
30	Conductor Impedance/1000'		Conductor Impedance for this segment	
31	Z1 & Z2	Z0	Z1 & Z2	Z0
32				
33	.0409+.1167j	.1296+.3576j	0.0216+0.0616j	0.0684+0.1888j
34	.0409+.1167j	.1296+.3576j	0.0216+0.0616j	0.0684+0.1888j
35	.0409+.1167j	.1296+.3576j	0.0216+0.0616j	0.0684+0.1888j
36	.0409+.1167j	.1296+.3576j	0.0216+0.0616j	0.0684+0.1888j
37	.0409+.1167j	.1296+.3576j	0.0216+0.0616j	0.0684+0.1888j
38	.0409+.1167j	.1296+.3576j	0.0216+0.0616j	0.0684+0.1888j
39	.0409+.1167j	.1296+.3576j	0.0216+0.0616j	0.0684+0.1888j
40	.0409+.1167j	.1296+.3576j	0.0216+0.0616j	0.0684+0.1888j
41	.0409+.1167j	.1296+.3576j	0.0216+0.0616j	0.0684+0.1888j
42	.0409+.1167j	.1296+.3576j	0.0216+0.0616j	0.0684+0.1888j
43	.0409+.1167j	.1296+.3576j	0.0216+0.0616j	0.0684+0.1888j
44	.0580+.1206j	.1408+.3615j	0.0306+0.0637j	0.0743+0.1909j
45	.0580+.1206j	.1408+.3615j	0.0306+0.0637j	0.0743+0.1909j
46	.0580+.1206j	.1408+.3615j	0.0306+0.0637j	0.0743+0.1909j
47	.0580+.1206j	.1408+.3615j	0.0306+0.0637j	0.0743+0.1909j
48	.0580+.1206j	.1408+.3615j	0.0306+0.0637j	0.0743+0.1909j
49	.0580+.1206j	.1408+.3615j	0.0306+0.0637j	0.0743+0.1909j

Fig. 9. Calculation of Circuit Segment Impedance

The segment impedances are then accumulated in Columns H and I, shown in Fig. 10, to give the total conductor impedance for the line at the end of each segment. These data are used in the impedance-based method. In Columns J and K, shown in Fig. 10, the secondary impedance of the substation transformer is added to the conductor impedance to yield the total circuit impedance. This result is used in the current-based method.

	H	I	J	K
30	Cumulative Conductor Impedance		Total Impedance with Transformer	
31	Z1 & Z2	Z0	Z1 & Z2	Z0
32				
33	0.0216+0.0616j	0.0684+0.1888j	0.0542+0.7943j	0.101+0.9215j
34	0.0432+0.1232j	0.1369+0.3776j	0.0758+0.8559j	0.1694+1.1103j
35	0.0648+0.1849j	0.2053+0.5664j	0.0973+0.9175j	0.2378+1.2991j
36	0.0864+0.2465j	0.2737+0.7553j	0.1189+0.9791j	0.3063+1.4879j
37	0.108+0.3081j	0.3421+0.9441j	0.1405+1.0407j	0.3747+1.6767j
38	0.1296+0.3697j	0.4106+1.1329j	0.1621+1.1024j	0.4431+1.8655j
39	0.1512+0.4313j	0.479+1.3217j	0.1837+1.164j	0.5116+2.0543j
40	0.1728+0.4929j	0.5474+1.5105j	0.2053+1.2256j	0.58+2.2431j
41	0.1944+0.5546j	0.6159+1.6993j	0.2269+1.2872j	0.6484+2.432j
42	0.216+0.6162j	0.6843+1.8881j	0.2485+1.3488j	0.7169+2.6208j
43	0.2375+0.6778j	0.7527+2.0769j	0.2701+1.4104j	0.7853+2.8096j
44	0.2682+0.7415j	0.8271+2.2678j	0.3007+1.4741j	0.8596+3.0005j
45	0.2988+0.8051j	0.9014+2.4587j	0.3314+1.5378j	0.934+3.1913j
46	0.3294+0.8688j	0.9757+2.6496j	0.362+1.6015j	1.0083+3.3822j
47	0.36+0.9325j	1.0501+2.8404j	0.3926+1.6651j	1.0826+3.5731j
48	0.3907+0.9962j	1.1244+3.0313j	0.4232+1.7288j	1.157+3.7639j
49	0.4213+1.0599j	1.1988+3.2222j	0.4539+1.7925j	1.2313+3.9548j

Fig. 10. Calculation of Cumulative Impedance

D. Current-Based Method

The available fault current at the end of each segment of the circuit is calculated in Columns L through O, as shown in Fig. 11. The values of fault current for single-phase-to-ground (Φ-to-▼), phase-to-phase (Φ-to-Φ), phase-to-phase-to-ground (Φ-to-Φ-to-▼), and three-phase (3Φ) faults are each calculated using the equations shown in Table II and provided in Appendix D. The value for *E* is the nominal single-phase-to-ground voltage shown in C6 of Fig. 5.

TABLE II
EQUATIONS FOR DETERMINING THE FAULT CURRENT FOR VARIOUS FAULT TYPES

Fault Type	Equation
Φ-to-▼	3 • E/(Z1 + Z2 + Z0)
Φ-to-Φ	√3 • E/(Z1 + Z2)
Φ-to-Φ-to-▼	E/(Z1 + Z0 • Z2/(Z0 + Z2)) • (–Z2/(Z0 + Z2) + a^2 – a • Z0/(Z0 + Z2)) where a = 1∠120°
3Φ	E/Z1

The calculated values shown in Columns L through O in Fig. 11 can be compared to the measured data, provided that the fault type is known. Note that both the fault type and fault currents in each phase are available in the event summary shown in Fig. 4.

	L	M	N	O
30	Fault Current Amps			
31	Φ to ▼	Φ to Φ	Φ-Φ-▼	3Φ
32				
33	8576	7832	4022	9044
34	7605	7257	3731	8380
35	6827	6758	3480	7804
36	6191	6322	3260	7300
37	5662	5937	3066	6856
38	5215	5596	2894	6462
39	4833	5291	2740	6110
40	4502	5018	2601	5794
41	4214	4771	2475	5509
42	3960	4546	2361	5250
43	3734	4342	2257	5014
44	3526	4145	2156	4786
45	3340	3964	2063	4577
46	3172	3798	1978	4385
47	3020	3645	1899	4209
48	2882	3503	1827	4045
49	2756	3372	1759	3894

Fig. 11. Calculation of Available Fault Current

E. Taps

Tables similar to those in Fig. 8, Fig. 9, Fig. 10, and Fig. 11 are built for each of the taps off of the main circuit. Fayetteville PWC color-coded the tap locations for each circuit and added driving directions to make the spreadsheet easier to use. Image of the complete spreadsheet showing the taps for Circuit 2-925 is included in Appendix E.

F. Impedance-Based Method

The applied relays use the modified Takagi method to locate faults, which requires line impedance data in secondary ohms. This subsection shows how Fayetteville PWC calculates the relay line impedance settings and how to interpret the fault location estimate from the relay.

Enter the largest conductor impedance from the cumulative conductor impedances into L54 and N54 to implement the impedance-based method, shown merged with their adjacent cells in Fig. 12. The largest impedance could be either on the main circuit or a tap.

The relay settings used for fault location are then calculated from these largest impedances, as shown in Fig. 12. The largest positive-sequence impedance, Z1, is put into polar form and multiplied by the CT/PT ratio to derive secondary ohms. The result is shown in Z1MAG (Q52) and Z1ANG (Q53). The largest zero-sequence impedance, Z0, is put into polar form and multiplied by the CT/PT ratio to derive secondary ohms. The result is shown in Z0MAG (Q54) and Z0ANG (Q55). The line length, LL (Q56), is set to 100.00. This does not represent the actual length but rather 100 percent of the maximum impedance.

	L	M	N	O	P	Q
51	CUMULATIVE CONDUCTOR IMPEDANCE - LARGEST VALUES				SETTING	VALUE
52	Sum of Z1		Sum of Z0		Z1MAG	2.28
53	R-1+jX-1		R-tot+jX-tot		Z1ANG	68.32
54	0.4213+1.0599j		1.1988+3.2222j		Z0MAG	6.88
55					Z0ANG	69.59
56					LL	100.00

Fig. 12. Calculation of Relay Settings

The magnitude of the cumulative conductor impedance from Fig. 10 is calculated and entered into Row P in Fig. 13. This is then converted to a percentage of total conductor impedance by comparing it to the setting Z1MAG in Column Q. This "location" can be compared to the location in the event summary (Fig. 4) to select the segment where the fault might be found. There could be more than one possible location on the main circuit or the taps.

	P	Q
31	Conductor Z1	Location
32		
33	0.07	5.72
34	0.13	11.45
35	0.20	17.18
36	0.26	22.90
37	0.33	28.62
38	0.39	34.35
39	0.46	40.07
40	0.52	45.79
41	0.59	51.53
42	0.65	57.25
43	0.72	62.97
44	0.79	69.13
45	0.86	75.29
46	0.93	81.46
47	1.00	87.64
48	1.07	93.82
49	1.14	100.00

Fig. 13. Impedance-Based Fault Location

V. Gathering and Validation of Field Data

During October and November 2016, Fayetteville PWC gathered relay event report data for six faults. Using the event report data, personnel assigned a fault location to the faults based on call-in information. The applied relay requires two full cycles of event data to provide valid fault location information. Three of the collected event reports met that criteria.

Based on this information, the authors loaded calculated relay settings for Z1, Z0, and LL (Fig. 12) into a relay in a laboratory and replayed the event data to the relay using a relay test set.

The results from the replayed events, including causes and fault currents, are shown in Table III.

TABLE III
RESULTS FROM REPLAYED EVENT FILES

			Fault Current (A)			
Circuit	**Cause**	**Type**	**A**	**B**	**C**	**G**
2-925	Squirrel	B-G	68	2,539	85	2,503
3-936	Tree	A-G	3,751	211	2,814	3,303
5-917	Squirrel	B-G	49	2,956	77	2,941

The resulting fault locations from the current- and impedance-based methods as compared to the estimated location due to call-in data are shown in Table IV. In each case, there was only one possible fault location on the line based on the fault location data. The current-based method was not able to locate two faults because the fault current in Table III is less than the available phase-to-ground fault current at the end of the line.

TABLE IV
FAULT LOCATION FROM REPLAYED EVENT FILES

		Estimated Fault Location (miles)		
Circuit	**Length**	**Call-In**	**Current**	**Impedance**
2-925	1.7	1.0	?	1.8
3-936	2.3	1.3	1.2	0.9
5-917	2.4	1.4	?	1.5

VI. OBSERVATIONS REGARDING FAULT LOCATION METHODS

Based on the experience to date, this section discusses some of the authors' observations about the two methods.

All of the faults had a fairly high fault resistance, so fault locations for two out of the three events could not be detected using the current-based method. The event on Circuit 3-936 had sufficient fault current to determine a fault location and proved to be reasonably accurate, even more so than the impedance-based method. This seems questionable because one would expect the current-based method to overreach the fault because of the resistance of the tree and that the impedance-based method should be the more accurate method for this case. However, three events are certainly not a statistically significant sample.

The spreadsheets have a possibility of multiple fault locations for tapped lines. Fault location accuracy can be improved by placing faulted circuit indicators on tapped lines. Fayetteville PWC does not employ faulted circuit indicators. Both fault locations that were reasonably accurate in Table IV could only have been in one location on the distribution circuit.

None of the faults in the collected data were permanent faults, and all had a fairly high fault resistance. The testing did not demonstrate the accuracy of methods for permanent faults.

The lines at Fayetteville PWC are short and consist of large conductors. This makes them nearly homogeneous, as shown for Circuit 2-925 in Fig. 14. The nonhomogeneity should not introduce much error into the impedance-based fault location.

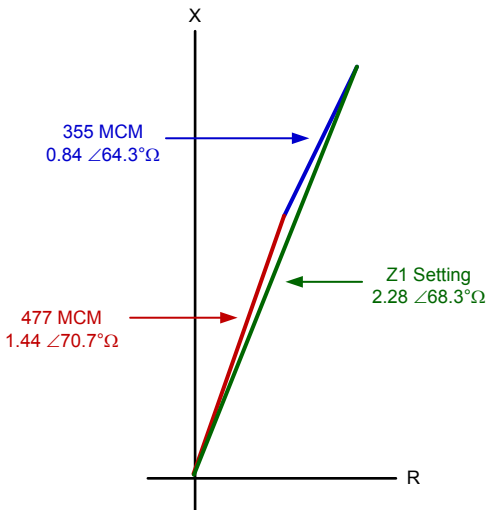

Fig. 14. Near Homogeneity of Positive-Sequence Line Impedance

The testing did not demonstrate the accuracy of methods for longer distribution lines or along smaller conductors. It is expected that the impedance-based method, as applied, may not work as well when lines reduce down to smaller conductors with higher X/R ratios and greater nonhomogeneity.

A few of the collected events were for trips on the fast curve during the first reclose. These events should be ignored for fault location because a recloser often closes in and trips on a second fast operation due to inrush current [9].

The current-based method in the spreadsheet does not include the system impedance. Adding the positive-sequence system impedance into Z1 and Z2 should make the current-based method slightly more accurate for a low-resistance fault. If the system impedance is not known, it can be measured using event data from the relay.

Looking at Fig. 15, the total system impedance can be measured as (10).

$$Z_{SI} + Z_{T1} = Z_{S2} + Z_{T2} = \frac{-V_2}{I_{S2}} \tag{10}$$

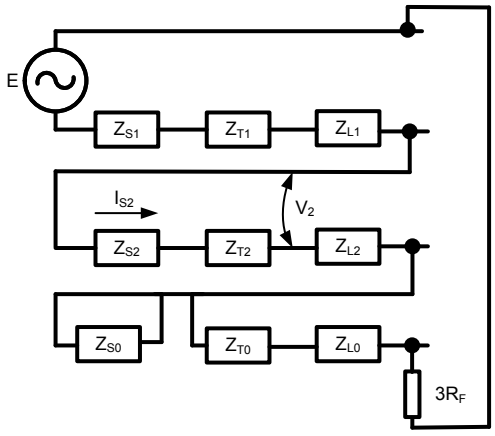

Fig. 15. Sequence Diagram of a Single-Line-to-Ground Fault

V2 and I2 from the Circuit 2-925 event in Fig. 16 can be used to calculate (11).

$$Z_{S1} + Z_{T1} = \frac{-V_2}{I_{S2}} = \frac{300\angle 180°}{346.8\angle 92.4°} = 0.87\angle 87.6°\,\Omega \quad (11)$$

Subtracting out the transformer impedance yields (12).

$$Z_{S1} = \frac{-V_2}{I_{S2}} - Z_{T1} = 0.87\angle 87.6° - 0.73\angle 87.5° = 0.14\angle 88°\,\Omega \quad (12)$$

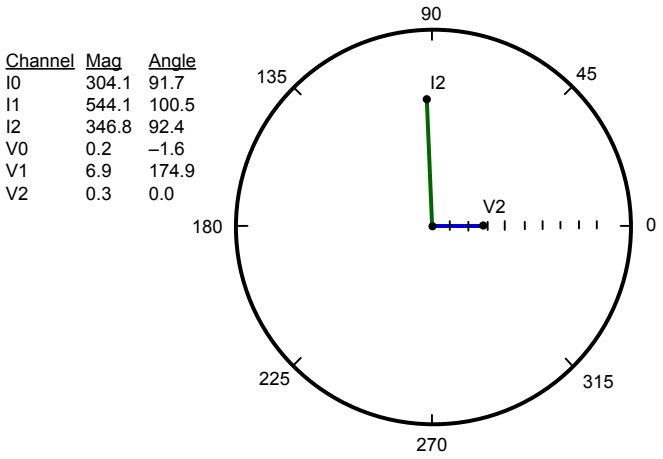

Fig. 16. V2 and I2 From Circuit 2-925 Event

The question was raised by Fayetteville PWC as to the effect of varying pole configurations on circuit impedance because it was not considered in the model and their GPS information does not include the pole configurations of the line segments. As shown in Table V, the impact of the pole configuration (using a 336 ACSR phase conductor) is not insignificant but is difficult to account for and not usually included. Impedances could be increased by a reasonable average to account for them if desired. The varying pole configurations are included in Appendix B, and a sample calculation for horizontal conductors a with neutral below is included in Appendix C.

TABLE V
CHANGE IN IMPEDANCE WITH VARYING POLE CONFIGURATIONS

Pole Configuration	Impedance Increase (%)	
	Z1/Z2	Z0
Horizontal with neutral below	+3.09	+4.39
Vertical conductors	+1.16	+8.78
Horizontal with in-line neutral	+2.89	+4.39
Pole-top insulators with neutral below	+4.10	+9.76

More sophisticated methods for finding faults on nonhomogeneous lines using impedance-based methods have been suggested [6]; however, they would be difficult to implement in real time using something like the simple, straightforward spreadsheet discussed in this paper.

The method would have limited usefulness for faults cleared by a downline fast-blowing or current-limiting fuse. Because these faults are less than two cycles long, they would not provide enough data for an accurate impedance-based fault location. Looking at the event summary data may not provide sufficient data for the current-based method either. This is evident from the raw and filtered event reports from [9] and shown in Fig. 17 and Fig. 18. Fig. 17 shows the raw event of a 10X fuse operation, while Fig. 18 shows the filtered event. The large current spike appears much lower after going through the one-cycle cosine filter used in the relay. This filtered current would be the current reported in the event summary. It could be useful to pull the raw event report to look at the fault current magnitude to help determine the location of a momentary fault.

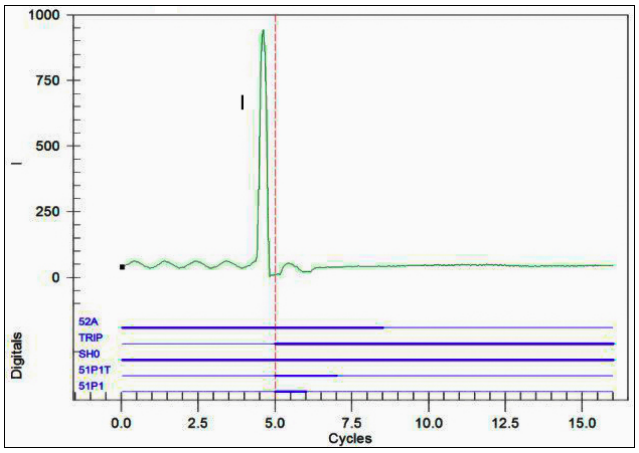

Fig. 17. Raw Event Report for Fuse Blowing

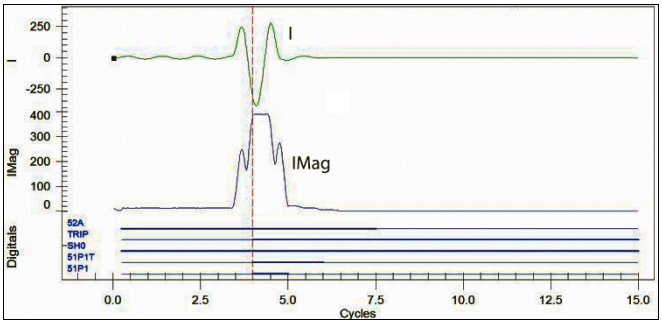

Fig. 18. Filtered Event Report for Fuse Blowing

The current magnitude method may be somewhat affected by dc offset. The current magnitude recorded in the event summary is the maximum current seen by the relay. This magnitude may include the true fault current plus some overshoot due to dc offset and filtering performed by the relay.

VII. Conclusion

The current-based and impedance-based methods are both useful for finding faults on a distribution line. They can be implemented using information from a microprocessor-based relay and a simple spreadsheet, making both methods accessible tools for the small utility. The impedance-based method should provide an improvement over the current-based method for faults with significant amounts of fault resistance. Although the spreadsheets used by Fayetteville PWC require more testing and data gathering and perhaps some adjustment to improve accuracy and determine when they are best applied, their design and structure form a good basis for other small utilities to develop their own fault location methods.

VIII. Appendix A: Formulas Used for Complex Equations in the Spreadsheet

The following formulas are used for complex equations in Fig. 8, Fig. 9, Fig. 10, Fig. 11, Fig. 12, and Fig. 13.

Cell	Formula
B11	COMPLEX(C11*COS(ATAN(C8)),C11*SIN(ATAN(C8)),"j")
F33[1]	IMPRODUCT($A33,D33,5.28)
G33[1]	IMPRODUCT($A33,E33,5.28)
H33[1]	IMSUM(H33,F33)
I33[1]	IMSUM(I33,G33)
J33[1]	IMSUM(H33,$C$12)
K33[1]	IMSUM(I33,$C$12)
L33[1]	$C$6*3/IMABS(IMSUM(J33,J33,K33))
M33[1]	SQRT(3)*$C$6/(2*IMABS(J33))
N33[1]	IMABS(IMDIV($C$6,IMPRODUCT(IMSUM(J33,IMPRODUCT(K33,IMDIV(J33,IMSUM(K33,J33)))),IMSUB(IMSUB(1,IMPRODUCT(COMPLEX(-0.5,-0.866,"j"),IMDIV(J33,IMSUM(K33,J33)))),IMPRODUCT(COMPLEX(-0.5,0.866,"j"),IMDIV(J33,IMSUM(K33,J33)))))))
O33[1]	$C$6/IMABS(J33)
P33[1]	IMABS(H33)
Q33[1,2]	P33/P$49*100
Q52[3]	IMABS(L54)*$C$10/$C$9
Q53[3]	IMARGUMENT(L54)*180/3.14159
Q54[3]	IMABS(N54)*$C$10/$C$9
Q55[3]	IMARGUMENT(N54)*180/3.14159

Footnotes:

1. Copy this formula down through the bottom of this column.
2. Cell P49 is the cell with the maximum Conductor Z1 Magnitude in Column P.
3. The magnitudes and angles of the maximum Cumulative Conductor Impedances, Z1 and Z0, are included in Columns H and I, respectively.

The figures in the paper rounded complex numbers to four digits. This was accomplished using the COMPLEX (ROUND(IMREAL(F33),4),ROUND(IMAGINARY(F33),4), "j") formula, with Cell F33 as an example.

IX. Appendix B: Analyzed Pole Configurations

Fig. 19, Fig. 20, Fig. 21, and Fig. 22 illustrate varying pole configurations.

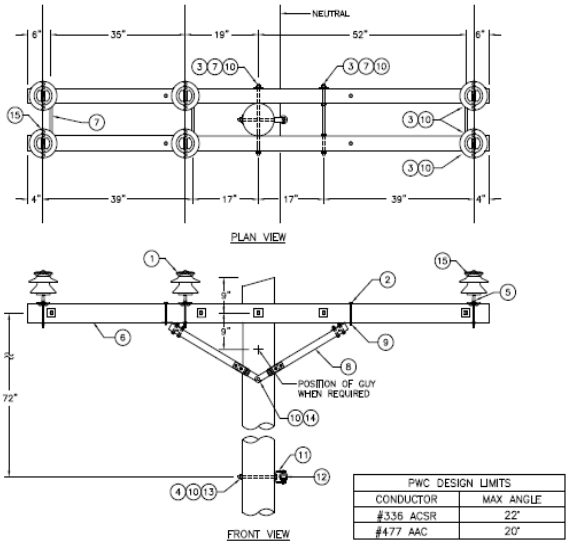

Fig. 19. Horizontal Conductors With Neutral Below

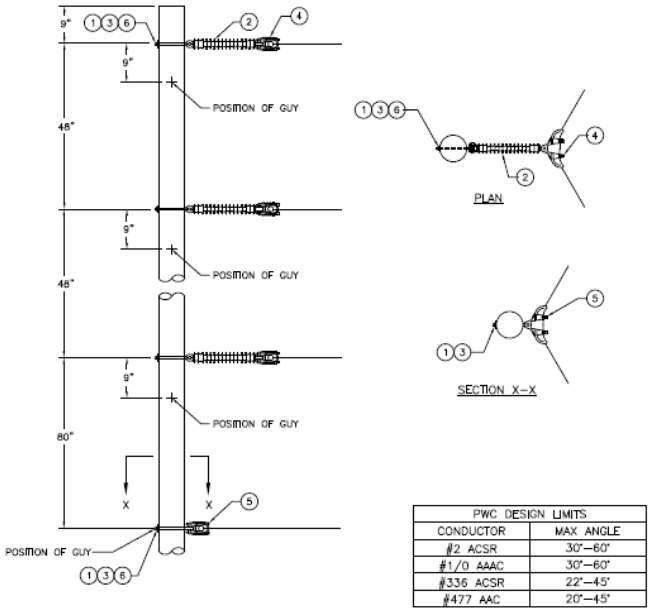

Fig. 20. Vertical Conductors

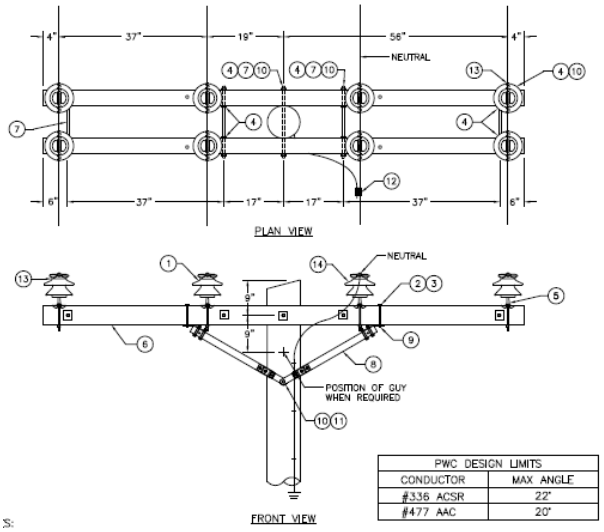

Fig. 21. Horizontal Conductors With In-Line Neutral

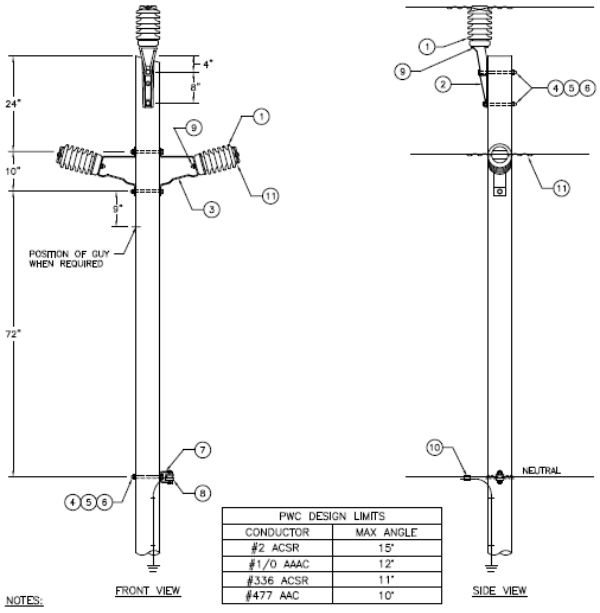

Fig. 22. Pole-Top Insulators With Neutral Below

X. Appendix C: Sample Calculation of Circuit Impedance of Horizontal Line With Neutral Below

This paper examined the effect of mutual inductance between conductors to determine if its impact was significant enough to include in line impedance calculations. This appendix describes the mathematical approach used to calculate sequence impedances for an example installation.

First, a tower structure used by the utility was selected to provide the geometry of the line spacing. This geometry had the three-phase conductors spaced horizontally and the neutral conductor lower on the pole. A diagram detailing the tower structure is shown in Fig. 19.

Next, typical resistance and geometric mean radius (GMR) values were retrieved for the conductors. A 336 ACSR phase conductor with a 4/0 neutral conductor was one of the pairings used by the utility and was chosen for this example. The resistance and GMR values used are listed in Table VI [10].

Table VI
Conductor Parameters

Conductor	Resistance (Ω per mile)	GMR (feet)
336,400 26/7 ACSR	0.3060	0.0244
4/0 6/1 ACSR	0.5920	0.0180

Using these line parameters, the self-impedance of each conductor, *i*, was calculated using the modified Carson's equation in (13) [10].

$$\hat{z}_{ii} = r_i + 0.0953 + j0.12134\left(\ln\frac{1}{GMR_i} + 7.93402\right)\Omega \text{ per mi.} \quad (13)$$

where:

r_i is the resistance (Ω per mile).

GMR_i is the GMR of the conductor (feet).

The mutual impedance between each conductor pair, *i* and *j*, was then calculated using the modified Carson's equation in (14) [10].

$$\hat{z}_{ij} = 0.0930 + j0.12134\left(\ln\frac{1}{D_{ij}} + 7.93402\right)\Omega \text{ per mi.} \quad (14)$$

where D_{ij} is the distance between each conductor pair (feet).

In (13) and (14), the frequency is assumed to be 60 Hz, and the earth resistivity is set equal to 100 Ω-m.

These self- and mutual-impedance values are assembled into a 4x4 impedance matrix, as shown in (15).

$$\hat{Z} = \begin{bmatrix} \hat{z}_{aa} & \hat{z}_{ab} & \hat{z}_{ac} & \hat{z}_{an} \\ \hat{z}_{ba} & \hat{z}_{bb} & \hat{z}_{bc} & \hat{z}_{bn} \\ \hat{z}_{ca} & \hat{z}_{cb} & \hat{z}_{cc} & \hat{z}_{cn} \\ \hat{z}_{na} & \hat{z}_{nb} & \hat{z}_{nc} & \hat{z}_{nn} \end{bmatrix} \quad (15)$$

Using the Kron reduction technique [10], (15) is reduced to a 3x3 matrix, shown in (16), which is the final phase impedance matrix describing the three-phase line.

$$Z_{abc} = \begin{bmatrix} z_{aa} & z_{ab} & z_{ac} \\ z_{ba} & z_{bb} & z_{bc} \\ z_{ca} & z_{cb} & z_{cc} \end{bmatrix}\Omega \text{ per mi.} \quad (16)$$

By using the technique of symmetrical components, the phase-impedance matrix is transformed into the sequence-impedance matrix using (17).

$$Z_{012} = [A_s]^{-1}[Z_{abc}][A_s] \quad (17)$$

where $[A_s]$ is the symmetrical components transformation matrix.

The sequence-impedance matrix is (18).

$$Z_{012} = \begin{bmatrix} z_{00} & z_{01} & z_{02} \\ z_{10} & z_{11} & z_{12} \\ z_{20} & z_{21} & z_{22} \end{bmatrix}\Omega \text{ per mi.} \quad (18)$$

In (18), position (1,1) is the zero-sequence impedance, position (2,2) is the positive-sequence impedance, and position (3,3) is the negative-sequence impedance.

The sequence-impedance matrix in (19) was produced from the line parameters and conductor geometry in this example.

$$Z_{012} = \begin{bmatrix} 0.7313 + j2.0106 & 0.0313 + j0.0104 & 0.0352 + j0.0131 \\ -0.0352 + j0.0131 & 0.3060 + j0.6610 & -0.0758 + j0.0102 \\ 0.0313 + j0.0104 & 0.0758 + j0.0102 & 0.3060 + j0.6610 \end{bmatrix} \Omega \text{ per mi.} \quad (19)$$

Table VII shows a comparison between these values and the sequence impedances that do not account for mutual coupling in polar form.

TABLE VII
SEQUENCE-IMPEDANCE COMPARISON

	Positive	**Negative**	**Zero**
Mutual inductance ignored	0.7066∠64.32°	0.7066∠64.32°	2.05∠68.72°
Mutual inductance included	0.7284∠65.16°	0.7284∠65.16°	2.14∠70.01°
Magnitude percent difference	+3.09%	+3.09%	0%

XI. APPENDIX D: DERIVATION OF FAULT CURRENT EQUATIONS

The fault current equations are derived using the method of symmetrical components [11]. Fig. 23 shows the sequence diagram for a three-phase fault.

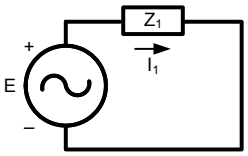

Fig. 23. Three-Phase Fault

Equation (20) is calculated using Ohm's law.

$$|I_f| = |I_1| = \left|\frac{E}{Z_1}\right| \quad (20)$$

I_A is used as the reference phase for Fig. 24 and Fig. 25.

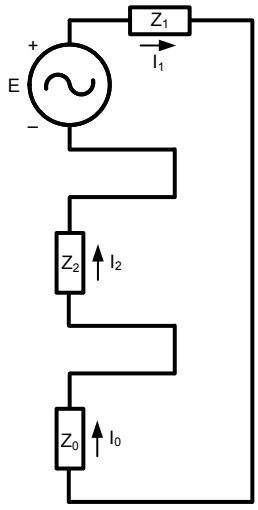

Fig. 24. Single-Phase-to-Ground Fault

The sequence diagram for a single-phase-to-ground fault in Fig. 24 can be used to calculate (21).

$$\begin{aligned} |I_f| &= |I_A| \\ &= |I_0 + I_1 + I_2| \\ &= \left|\frac{3E}{Z_0 + Z_1 + Z_2}\right| \end{aligned} \quad (21)$$

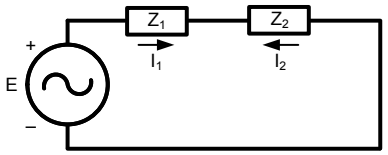

Fig. 25. Phase-to-Phase Fault

The sequence diagram for a phase-to-phase fault in Fig. 25 can be used to calculate (22).

$$\begin{aligned} |I_f| &= |I_B| \\ &= |I_0 + a^2 I_1 + a I_2| \\ &= |a^2 I_1 - a I_1| \\ &= \left|\frac{-j\sqrt{3}E}{Z_1 + Z_2}\right| \\ &= \left|\frac{\sqrt{3}E}{Z_1 + Z_2}\right| \end{aligned} \quad (22)$$

where a = 1 ∠120°.

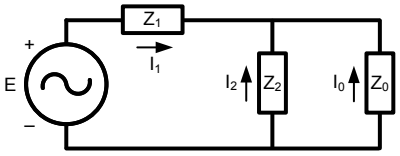

Fig. 26. Phase-to-Phase-to-Ground Fault

The sequence diagram for a phase-to-phase-to-ground fault in Fig. 26 can be used to calculate (23) and (24).

$$\begin{aligned} |I_f| &= |I_B| \\ &= |I_0 + a^2 I_1 + a I_2| \end{aligned} \quad (23)$$

$$I_1 = \frac{E}{Z1 + \dfrac{Z0 \bullet Z2}{Z0 + Z2}}$$

$$I_2 = -I_1 \frac{Z0}{Z0 + Z2} \quad (24)$$

$$I_0 = -I_1 \frac{Z2}{Z0 + Z2}$$

Substituting these back into (23) yields (25).

$$|I_f| = \left| \frac{E}{Z1 + \dfrac{Z0 \bullet Z2}{Z0 + Z2}} \left(-\frac{Z2}{Z0 + Z2} + a^2 - a \frac{Z0}{Z0 + Z2} \right) \right| \quad (25)$$

where a = 1∠120°.

ARRAN PARK SUBSTATION

Transformer Size (MVA)	20
Impedance (Z%)	8.56
Voltage Φ-Φ (LV)	13090
Voltage Φ-▼ (LV) Grd'Y	7560
Voltage Φ-▼ (LV) after LTC	7200
Voltage (HV) Delta	67000
X/R ratio	22.5
PT Ratio	60
CT Ratio	120
Zmagnitude (Ω)	0.73
Zcomplex (Ω)	0.0326+0.7326j
Ifault (A)	10302

	R+jX/1000'	
Wire Size	Z1& Z2	Z0
477 w/ 4/0-N	.0409+.1167j	.1296+.3576j
477 w/ 2/0-N	.0409+.1167j	.1504+.3820j
477 w/ 1/0-N	.0409+.1167j	.1614+.4008j
355 w/ 4/0-N	.0580+.1206j	.1408+.3615j
355 w/ 2/0-N	.0580+.1206j	.1672+.3860j
355 w/ 1/0-N	.0580+.1206j	.1784+.4047j
2/0AL w/ 2/0-N	.1695+.1566j	.2389+.4595j
1/0AL w/ 1/0-N	.2121+.1595j	.3447+.4794j

FEEDER #2

LEAVING SUBSTATION GO NORTH ON ARRAN CIR, TURN RIGHT ON RAEFORD RD UNTIL OPEN SWITCH AFTER DURANT DR

			Conductor Impedance/1000'		Conductor Impedance for this segment		Cumulative Conductor Impedance		Total Impedance with Transformer		Fault Current Amps					
Segment Length	Total Distance (miles)	Wire Size	Z1& Z2	Z0	Z1& Z2	Z0	Z1& Z2	Z0	Z1& Z2	Z0	Φ to ▼	Φ to Φ	Φ-Φ-▼	3Φ	Conductor Z1	Location
0.1	0.1	477 W/ 4/0-N	.0409+.1167j	.1296+.3576j	0.0216+0.0616j	0.0684+0.1888j	0.0216+0.0616j	0.0684+0.1888j	0.0542+0.7943j	0.1101+0.9215j	8576	7832	4022	9044	0.07	5.72
0.1	0.2	477 W/ 4/0-N	.0409+.1167j	.1296+.3576j	0.0216+0.0616j	0.0684+0.1888j	0.0432+0.1232j	0.1369+0.3776j	0.0758+0.8553j	0.1694+1.1103j	7605	7257	3731	8380	0.13	11.45
0.1	0.3	477 W/ 4/0-N	.0409+.1167j	.1296+.3576j	0.0216+0.0616j	0.0684+0.1888j	0.0648+0.1849j	0.2053+0.5664j	0.0973+0.9175j	0.2378+1.2391j	6827	6758	3480	7804	0.20	17.18
0.1	0.4	477 W/ 4/0-N	.0409+.1167j	.1296+.3576j	0.0216+0.0616j	0.0684+0.1888j	0.0864+0.2465j	0.2737+0.7553j	0.1189+0.9791j	0.3063+1.4879j	6191	6322	3260	7300	0.26	22.90
0.1	0.5	477 W/ 4/0-N	.0409+.1167j	.1296+.3576j	0.0216+0.0616j	0.0684+0.1888j	0.1080+0.3081j	0.3421+0.9441j	0.1405+1.0407j	0.3747+1.6767j	5662	5937	3066	6856	0.33	28.62
0.1	0.6	477 W/ 4/0-N	.0409+.1167j	.1296+.3576j	0.0216+0.0616j	0.0684+0.1888j	0.1296+0.3697j	0.4106+1.1323j	0.1621+1.1024j	0.4431+1.8655j	5215	5596	2894	6462	0.39	34.35
0.1	0.7	477 W/ 4/0-N	.0409+.1167j	.1296+.3576j	0.0216+0.0616j	0.0684+0.1888j	0.1512+0.4313j	0.479+1.3217j	0.1837+1.164j	0.5116+2.0543j	4833	5291	2740	6110	0.46	40.07
0.1	0.8	477 W/ 4/0-N	.0409+.1167j	.1296+.3576j	0.0216+0.0616j	0.0684+0.1888j	0.1728+0.4929j	0.5474+1.5105j	0.2053+1.2256j	0.58+2.2431j	4502	5018	2601	5794	0.52	45.79
0.1	0.9	477 W/ 4/0-N	.0409+.1167j	.1296+.3576j	0.0216+0.0616j	0.0684+0.1888j	0.1944+0.5546j	0.6159+1.6993j	0.2269+1.2872j	0.6484+2.432j	4214	4771	2475	5509	0.59	51.53
0.1	1.0	477 W/ 4/0-N	.0409+.1167j	.1296+.3576j	0.0216+0.0616j	0.0684+0.1888j	0.216+0.6162j	0.6843+1.8881j	0.2485+1.3488j	0.7169+2.6208j	3960	4546	2361	5250	0.65	57.25
0.1	1.1	477 W/ 4/0-N	.0409+.1167j	.1296+.3576j	0.0216+0.0616j	0.0684+0.1888j	0.2375+0.6778j	0.7527+2.0769j	0.2701+1.4104j	0.7853+2.8036j	3734	4342	2257	5014	0.72	62.97
0.1	1.2	355 W/ 4/0-N	.0580+.1206j	.1408+.3615j	0.0306+0.0637j	0.0743+0.1909j	0.2682+0.7415j	0.8271+2.2678j	0.3007+1.4741j	0.8596+3.0005j	3526	4145	2156	4786	0.79	69.13
0.1	1.3	355 W/ 4/0-N	.0580+.1206j	.1408+.3615j	0.0306+0.0637j	0.0743+0.1909j	0.2988+0.8051j	0.9014+2.4587j	0.3314+1.5378j	0.934+3.1913j	3340	3964	2063	4577	0.86	75.29
0.1	1.4	355 W/ 4/0-N	.0580+.1206j	.1408+.3615j	0.0306+0.0637j	0.0743+0.1909j	0.3294+0.8688j	0.9757+2.6496j	0.362+1.6015j	1.0083+3.3822j	3172	3798	1978	4385	0.93	81.46
0.1	1.5	355 W/ 4/0-N	.0580+.1206j	.1408+.3615j	0.0306+0.0637j	0.0743+0.1909j	0.36+0.9325j	1.0501+2.8404j	0.3926+1.6651j	1.0826+3.5731j	3020	3645	1899	4209	1.00	87.64
0.1	1.6	355 W/ 4/0-N	.0580+.1206j	.1408+.3615j	0.0306+0.0637j	0.0743+0.1909j	0.3907+0.9962j	1.1244+3.0313j	0.4232+1.7288j	1.157+3.7639j	2882	3503	1827	4045	1.07	93.82
0.1	1.7	355 W/ 4/0-N	.0580+.1206j	.1408+.3615j	0.0306+0.0637j	0.0743+0.1909j	0.4213+1.0599j	1.1988+3.2222j	0.4539+1.7925j	1.2313+3.9548j	2756	3372	1759	3894	1.14	100.00

CUMULATIVE CONDUCTOR IMPEDANCE - LARGEST VALUES		SETTING	VALUE
Sum of Z1	Sum of Z0	Z1MAG	2.28
R-1+jX-1	R-tot+jX-tot	Z1ANG	68.32
0.4213+1.0599j	1.1988+3.2222j	Z0MAG	6.88
		Z0ANG	69.59
		LL	100.00

LEAVING SUBSTATION GO NORTH ON ARRAN CIR, TURN RIGHT ON RAEFORD RD, TURN LEFT ON BUNCE RD UNTIL DEADEND AFTER ST LOUIS ST

			Conductor Impedance/1000'		Conductor Impedance for this segment		Cumulative Conductor Impedance		Total Impedance with Transformer		Fault Current (A)					
Segment Length	Total Distance (miles)	Wire Size	Z1& Z2	Z0	Z1& Z2	Z0	Z1& Z2	Z0	Z1& Z2	Z0	Φ-▼	Φ-Φ	Φ-Φ-▼	3Φ	Conductor Z1	Location
0.1	0.2	477 W/ 4/0-N	.0409+.1167j	.1296+.3576j	0.0216+0.0616j	0.0684+0.1888j	0.0432+0.1232j	0.1369+0.3776j	0.0758+0.8553j	0.1694+1.1103j	7605	7257	3731	8380	0.13	11.45
0.1	0.3	477 W/ 4/0-N	.0409+.1167j	.1296+.3576j	0.0216+0.0616j	0.0684+0.1888j	0.0648+0.1849j	0.2053+0.5664j	0.0973+0.9175j	0.2378+1.2391j	6827	6758	3480	7804	0.20	17.18
0.1	0.4	355 W/ 1/0-N	.0580+.1206j	.1784+.4047j	0.0306+0.0637j	0.0942+0.2137j	0.0954+0.2485j	0.2995+0.7801j	0.128+0.9612j	0.332+1.5128j	6129	6302	3251	7277	0.27	23.34
0.1	0.5	355 W/ 1/0-N	.0580+.1206j	.1784+.4047j	0.0306+0.0637j	0.0942+0.2137j	0.126+0.3122j	0.3937+0.9938j	0.1586+1.0443j	0.4262+1.7264j	5556	5900	3049	6813	0.34	29.52
0.1	0.6	355 W/ 1/0-N	.0580+.1206j	.1784+.4047j	0.0306+0.0637j	0.0942+0.2137j	0.1567+0.3759j	0.4879+1.2075j	0.1892+1.1085j	0.5204+1.9401j	5078	5545	2870	6402	0.41	35.71
0.1	0.7	355 W/ 1/0-N	.0580+.1206j	.1784+.4047j	0.0306+0.0637j	0.0942+0.2137j	0.1873+0.4396j	0.5821+1.4212j	0.2198+1.1722j	0.6146+2.1538j	4675	5228	2711	6037	0.48	41.89
0.1	0.8	355 W/ 1/0-N	.0580+.1206j	.1784+.4047j	0.0306+0.0637j	0.0942+0.2137j	0.2179+0.5032j	0.6763+1.6348j	0.2505+1.2359j	0.7088+2.3675j	4330	4945	2567	5710	0.55	48.08
0.1	0.9	355 W/ 1/0-N	.0580+.1206j	.1784+.4047j	0.0306+0.0637j	0.0942+0.2137j	0.2485+0.5663j	0.7705+1.8485j	0.2811+1.2996j	0.803+2.5812j	4032	4690	2438	5415	0.62	54.27
0.1	1	355 W/ 1/0-N	.0580+.1206j	.1784+.4047j	0.0306+0.0637j	0.0942+0.2137j	0.2792+0.6306j	0.8647+2.0622j	0.3117+1.3632j	0.8972+2.7949j	3772	4459	2320	5149	0.69	60.47
0.1	1.1	355 W/ 1/0-N	.0580+.1206j	.1784+.4047j	0.0306+0.0637j	0.0942+0.2137j	0.3098+0.6943j	0.9588+2.2759j	0.3423+1.4263j	0.9914+3.0085j	3543	4249	2214	4907	0.76	66.66

LEAVING SUBSTATION GO NORTH ON ARRAN CIR, TURN RIGHT ON RAEFORD RD, TURN LEFT ON SKIBO RD UNTIL OPEN SWITCH

			Conductor Impedance/1000'		Conductor Impedance for this segment		Cumulative Conductor Impedance		Total Impedance with Transformer		Fault Current Amps					
Segment Length	Total Distance	Wire Size	Z1& Z2	Z0	Z1& Z2	Z0	Z1& Z2	Z0	Z1& Z2	Z0	Φ to ▼	Φ to Φ		3Φ Fault	Conductor Z1	Location
0.1	1.1	477 W/ 4/0-N	.0409+.1167j	.1296+.3576j	0.0216+0.0616j	0.0684+0.1888j	0.2375+0.6778j	0.7527+2.0769j	0.2701+1.4104j	0.7853+2.8036j	3734	4342	2257	5014	0.72	62.97
0.1	1.2	355 W/ 2/0-N	.0580+.1206j	.1672+.3860j	0.0306+0.0637j	0.0883+0.2038j	0.2682+0.7415j	0.841+2.2807j	0.3007+1.4741j	0.8736+3.0134j	3517	4145	2156	4786	0.79	69.13

XIII. Acknowledgements

The authors would like to acknowledge the contribution of David DesChamps of the City of Wilson, North Carolina, in helping to develop the fault location techniques currently employed by Fayetteville PWC.

XIV. References

[1] Y. Gong and A. Guzmán, "Distribution Feeder Fault Location Using IED and FCI Information," proceedings of the 64th Annual Conference for Protective Relay Engineers, College Station, TX, April 2011.

[2] K. Zimmerman and D. Costello, "Impedance-Based Fault Location Experience," 31st Annual Western Protective Relay Conference, Spokane, WA, October 2004.

[3] APPA, "Grants Awarded in Fall 2015" DEED Digest, Vol. 34, Issue 1, Winter 2015–16, pp. 8. Available: http://appanet.files.cms-plus.com/Deed/deeddigest-winter2015.pdf.

[4] J. I. Holbeck, "A Simple Method for Locating Ground Faults," *Electrical Engineering*, Vol. 63, No. 3, March 1944, pp. 89–92.

[5] Electric Power Research Institute (EPRI), "Distribution Fault Location: Field Data and Analysis," December 2006. Available: https://www.epri.com/#/pages/product/1012438/.

[6] E. O. Schweitzer, III, "A Review of Impedance-Based Fault Locating Experience," proceedings of the Northwest Electric Light & Power Association Conference, April 1988.

[7] IEEE Standard C37.114-2004, 2005, IEEE Guide for Determining Fault Location on AC Transmission and Distribution Lines.

[8] IEEE Standard 141-1993 (R1999), Recommended Practice for the Electric Power Distribution for Industrial Plants.

[9] L. Wright and L. Ayers, "Mitigation of Undesired Operation of Recloser Controls Due to Distribution Line Inrush," 68th Annual Conference for Protective Relay Engineers, College Station, TX, March 2015.

[10] W. Kersting, *Distribution System Modeling and Analysis*. CRC Press, Boca Raton, FL, 2012. Third Edition.

[11] E. O. Schweitzer, III, and S. E. Zocholl, "Introduction to Symmetrical Components," proceedings of the 30th Annual Western Protective Relay Conference, Spokane, WA, October 2003.

XV. Biographies

Thomas Covington received a BS in Electrical Engineering in 2010 from North Carolina Agricultural and Technical State University. From 2010 until 2015, he worked for Eaton Corporation as an applications engineer on the low-voltage motor control center product line. He joined Fayetteville Public Works Commission in 2015, where he is presently an electric systems engineer.

Tim Stankiewicz, P.E., holds a Bachelor's Degree in Electrical Engineering from the University of Central Florida and a Master's Degree in Business Administration from the University of Phoenix. Tim currently works for Fayetteville Public Works Commission. In addition to registration as a Professional Engineer in North Carolina, he is also a Member of the IEEE. He is an accomplished electrical engineer with more than 20 years of experience in the electric utility industry and more than 10 years of experience in project management. Tim possesses strong knowledge of operations, safety, and construction. During his tenure in the electric utility industry, Tim has worked for Nevada Power, Duke-Progress Energy, and ABB.

Rick Anderson, P.E., received a BS in Electrical Engineering in 1979 from the University of Central Florida. From 1979 until 1995, he worked for Duke-Progress Energy (formerly Carolina Power & Light) as a metering engineer, systems manager, and manager of distribution design. From 1995 through 2004, Rick was the manager of engineering and system planning for the City of Wilson, North Carolina. From 2004 through 2006, he was an owner of an electrical distributor company, which served electrical municipal systems and electrical cooperatives in five states. He joined the Fayetteville Public Works Commission in 2006 as manager of electrical engineering. Rick is a licensed Professional Engineer, Electrical Contractor, and General Building Contractor in North Carolina.

Larry Wright, P.E., received a BS in Electrical Engineering in 1982 from North Carolina State University. From 1982 until 2003, he worked for Duke Energy, designing nuclear, hydroelectric, and fossil-powered generating stations for Duke Energy and other utilities and independent power producers. From 2003 to 2005, Larry served as the subject matter expert on protective relaying for Duke Energy's generating stations. He joined Devine Tarbell Associates in 2005 as manager of electrical engineering, providing consulting services to the hydroelectric industry. In 2008, he joined Schweitzer Engineering Laboratories, Inc., where he is presently a field application engineer. Larry is a registered Professional Engineer in the state of North Carolina.

Brett M. Cockerham earned his B.S., summa cum laude, in 2014 and his M.Sc. in applied energy and electromechanical systems in 2016. Both degrees were awarded by the University of North Carolina at Charlotte. His graduate school research focused on power system frequency and frequency estimation methods. Brett joined Schweitzer Engineering Laboratories, Inc. in 2016 as a protection application engineer in Charlotte, North Carolina.